DEUTSCHES ELEKTRONEN – SYNCHROTRON
INSTITUT FÜR HOCHENERGIEPHYSIK

DESY 93-002
January 1993

Design of a Silicon Backward Tracking Detector and Trigger for the H1 Experiment at the ep Collider HERA

J. Bürger, U. Harder, H. Henschel, H. H. Kaufmann, M. Klein, P. Kostka,
W. Lange, H. Lippold, J. Meißner, T. Naumann, M. Winde, N. Wulff

Deutsches Elektronen-Synchrotron DESY
Institut für Hochenergiephysik IfH, Zeuthen

ISSN 0418-9833

PLATANENALLEE 6 · O-1615 ZEUTHEN

To be sure that your preprints are promptly included in the
HIGH ENERGY PHYSICS INDEX,
send them to (if possible by air mail):

DESY
Bibliothek
Notkestraße 85
W-2000 Hamburg 52
Germany

DESY-IfH
Bibliothek
Platanenallee 6
O-1615 Zeuthen
Germany

DESY 93-002
January 1993

ISSN 0418-9833

DESIGN OF A SILICON BACKWARD TRACKING DETECTOR AND TRIGGER FOR THE H1 EXPERIMENT AT THE ep COLLIDER HERA.

J. Bürger, U. Harder, H. Henschel, H.H. Kaufmann, M. Klein, P. Kostka, W. Lange, H. Lippold, J. Meißner, T. Naumann, M. Winde, N. Wulff

DESY Hamburg & Zeuthen, Germany

The material contained herein is an updated version of a talk held at the 1992 Nuclear Science Symposium in Orlando.

ABSTRACT

We describe a proposal to upgrade the existing H1 tracking detector by a semiconductor backward tracking telescope consisting of 8 beam concentric discs to measure the gluon and quark distribution functions at very low Bjorken *x*. Each disc comprises 3 planes of strip and pad Silicon detectors made of 4" wafers in order to determine the polar angle, the transverse momentum and to trigger on deep inelastically scattered electrons. The paper details the simulation work and the layout constraints on the semiconductors and it reviews the technical and electronics design of the trigger which has to cope with very high beam background rates and the HERA bunch crossing rate of 10.4*MHz*. A first phase of the project was approved by the H1 collaboration and will be operational in 1994.

1. INTRODUCTION

Recently the H1 collaboration has proposed to build a Backward Silicon Tracker (BST) in order to complement the tracking capabilities of the existing H1 detector down to very low scattering angles [1]. This device, in conjunction with an improved backward calorimeter [2], will enable detailed investigations of deep inelastic scattering $ep \rightarrow eX$ at small Bjorken $x \leq 10^{-4}$. It is intended to study the anticipated recombination and saturation effects in the gluon structure function which could qualitatively change our understanding of quark and gluon interactions.

The BST will provide a trigger on backward scattered electrons which will help to further reduce the H1 background trigger rate of beam halo and synchrotron radiation interactions.

The BST will consist of eight disk-shaped planes perpendicular to the beam, placed between 300*mm* and 1046*mm* off the nominal vertex in -z direction (i.e. direction of electron beam) and covering a radial area between 59*mm* and 120.4*mm*. Each plane will be equipped with three types of silicon sensors for measuring the polar angle, the transverse momentum and for triggering on charged particles. The BST will be built in two stages, BST(1) and BST(2), the first one comprising four planes only and being limited to the detection of the polar angle ϑ (including trigger).

2. PHYSICS REQUIREMENTS

We summarize the physics demands here - for a more detailed report see [1].

The BST shall be able to measure the tracks of most deep inelastic scattering events at a momentum transfer of about $Q^2 \geq 4 GeV^2$. Fig. 1. shows the appropriate kinematical distributions, where the dashed histograms represent the fraction of events recognized by the BST in comparison to the total number of deep inelastic events. The detectors ought to be sensitive in the polar angular range between 176° (where the beam pipe diameter sets a limit) and the innermost sensitive edge of the existing tracking detectors (about 167°). In order to allow the reconstruction of a track without external reference, e.g. without a reconstructed vertex, the BST must provide at least three hits for every angle within this range; thus its planes should be displaced along the beam axis following a geometric series (cf. chapter 3.1.2).

Since there is rather limited space available in the backward region of H1 for an improved calorimeter it is also desirable to measure the transverse momentum of the charged hadrons with the BST. Fig. 2 shows that the momentum measurement with the BST in the solenoid field can be superior to a calorimetric measurement below about 15*GeV* and down to

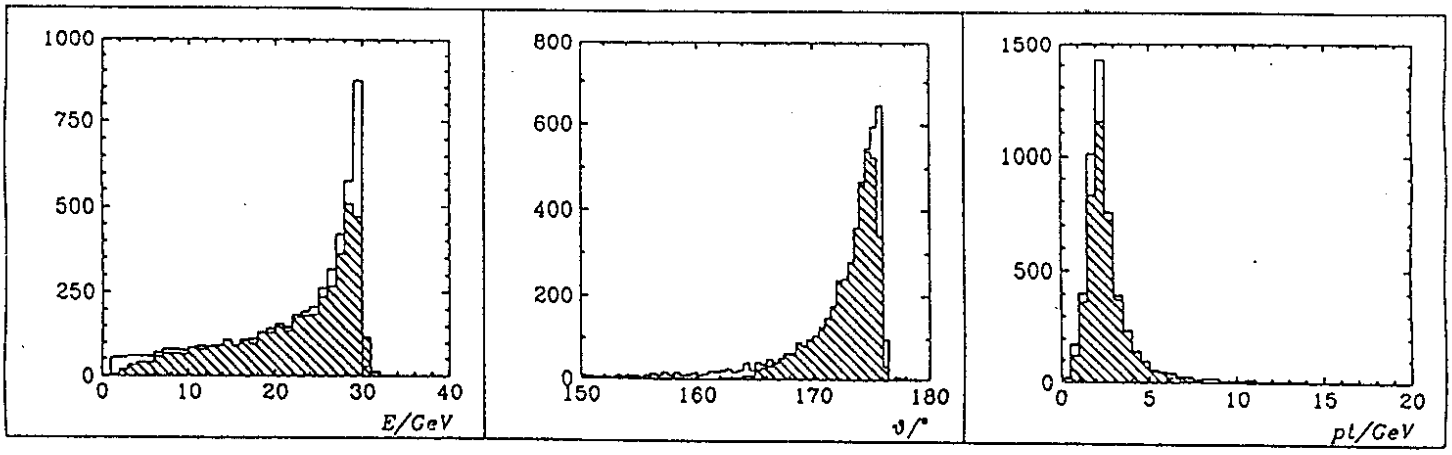

Figure 1: Kinematical distributions of deep inelastic events for $Q^2 \geq 4$ GeV² and $y \geq 0.01$. The dashed histograms show the distributions of reconstructed scattered electrons traversing at least 3 planes of BST(2).

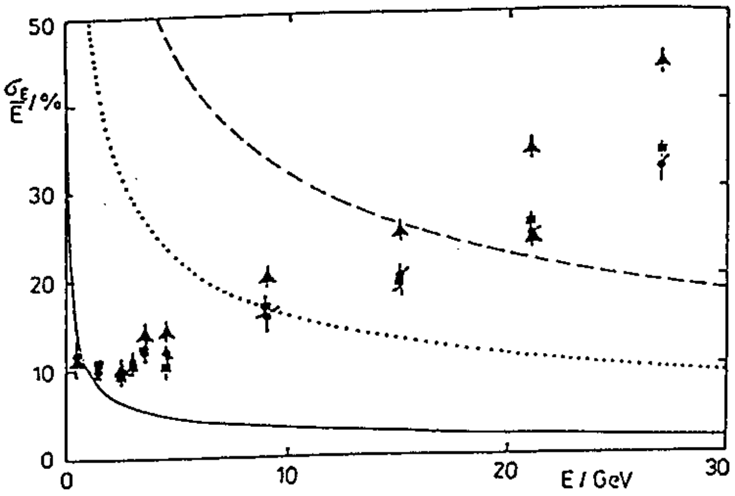

Figure 2: Energy resolutions for a sample of events in the BST. Points: resolutions achievable with the BST for different ϕ pitches (0.5, 1 and 3mrad); curves: calorimetric measurements with resolutions of 10, 50 and 100%/$\sqrt{E}$ (solid, dotted and dashed curve, resp.)

a few *GeV* where multiple scattering becomes dominant.

These demands result in a desired angular resolution of both the polar and the azimuthal measurement of about 1*mrad.*

Since the BST serves deep inelastic scattering physics mainly a dedicated trigger tagging single electrons in the considered angular area is highly desirable. This will in addition reject a valuable amount of background triggers which presently fake qualified events.

3. DESIGN CONSIDERATIONS

3.1 Physics Simulation

3.1.1 Basic Constraints

The Silicon Sensor technology implies a few constraints to which the detector design has to be adapted. These are for the BST:

- the available active area of a 4" Silicon wafer;
- the utilization of a standard, state-of-the-art detector technology since no time is available for considerable R&D;
- the need for a unique wafer layout regardless of the *z* position of a given sensor along the beam axis.

As a result of these constraints the principle structure of BST(1) (and BST(2)) was fixed (cf. fig. 3): each of the four

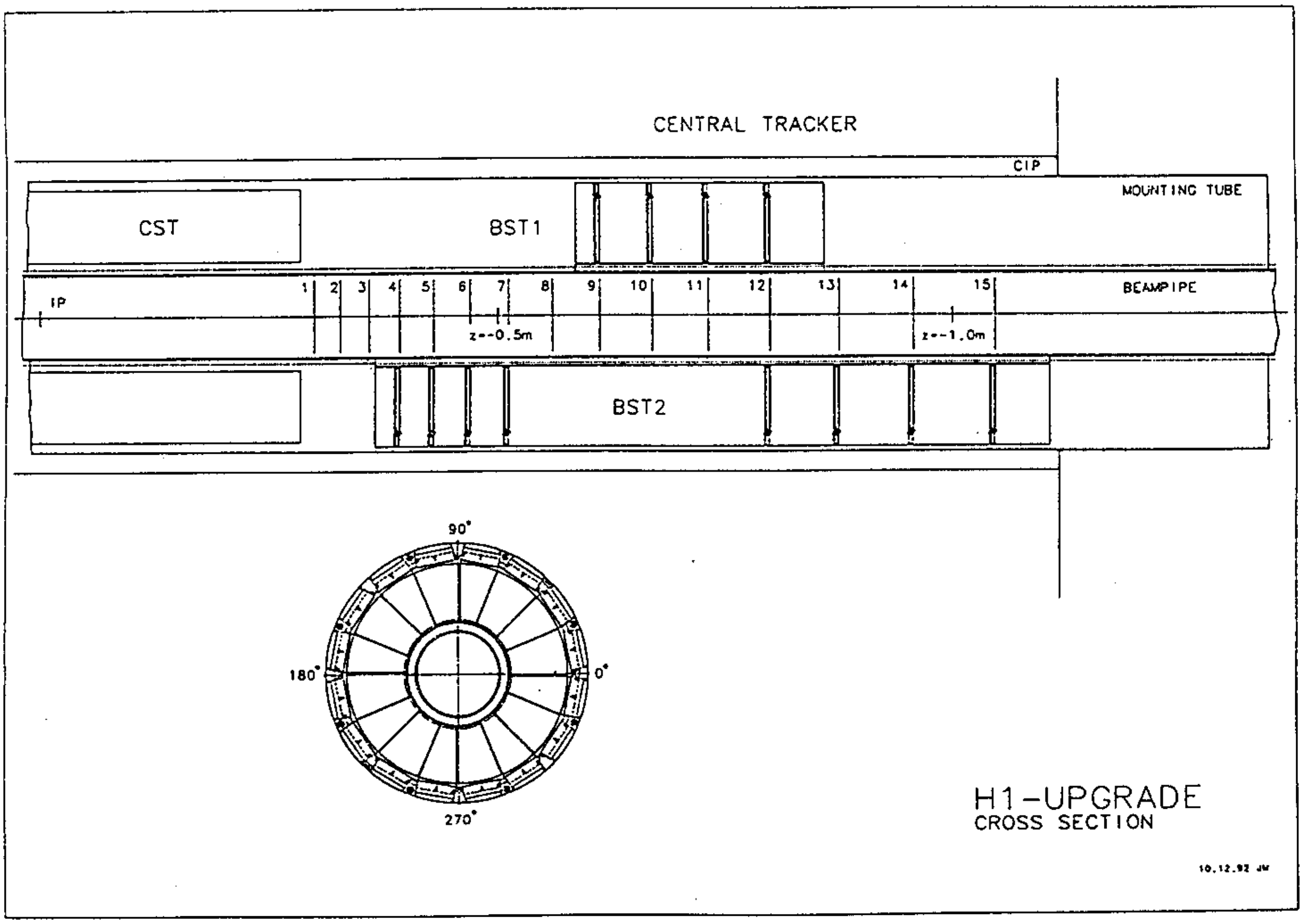

Figure 3: Structure of the BST (section along beam axis with BST(1) planes (top) and BST(2) planes (bottom); view of r-ϕ plane).

(eight) planes is a compound of two (three) dedicated layers which in turn consist of 16 staggered and overlapping wedge shaped sensors. Each layer has its individual task, measuring ϑ, ϕ or triggering, resp. The overlap between neighbouring wedges allows for an easy relative geometry calibration using the detector data themselves. All readout and biasing electronics are located at the outer circumference of the sensors.

3.1.2 Design Optimization

The design of the tracking sensors was more or less straight forward, starting from the required single coordinate resolution of $1mrad$ in the $r\phi$ plane. Both types of detectors show a strip diode pattern with strips at constant r and constant ϕ respectively, see fig. 4.

The design of the trigger sensor was subject to a rather extensive optimization process in order to keep the related trigger electronics reasonable simple. Note that the trigger has to be conform to the H1 'level 1', i.e. it has to be processed in parallel or pipelined within a $2\mu s$ interval keeping its dead time below the H1 bunch crossing sequence of approx. $96ns$.

- *Pointing Track Geometry*

The trigger should utilize a natural pointing track geometry with respect to the nominal interaction vertex. Thus the trigger sensors should be radially subdivided; the radii of the resulting rings must follow a geometric series (equation (1)) hence the positions of the planes along the beam axis (equation (2)) as well, cf. fig. 5. Starting values are the innermost radius of a sensor r_{min} which is defined by the beam pipe and the closest approach to the vertex z_{min} allowed by the proposed Central Silicon Tracking detector CST (see [1]).

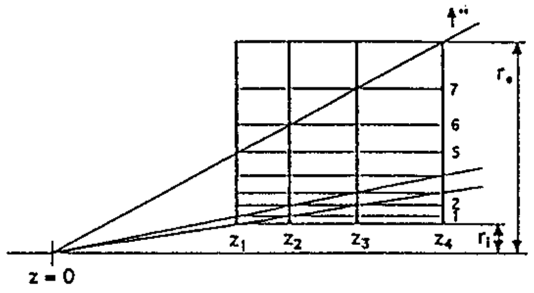

i	1	2	3	4	5	6	7	8	9	10	11	12	13	14	15
z/mm	-300	-328	-359	-392	-429	-469	-512	-560	-612	-670	-732	-800	-875	-957	-1046
BST (1)									•	•	•	•			
BST (2)				•	•	•	•					•	•	•	•

Figure 5: Pointing track geometry of the BST; possible z positions and those chosen for BST(1) and BST(2).

$$r_k = r_{min} \cdot \left(\frac{z_2}{z_1}\right)^k \tag{1}$$

$$z_{i+1} = z_i \cdot \sqrt[n]{\frac{r_{max}}{r_{min}}} \tag{2}$$

For reasons of the digital trigger processing electronics we chose $k = 8$; 12 consecutive z positions seem sensible. Not

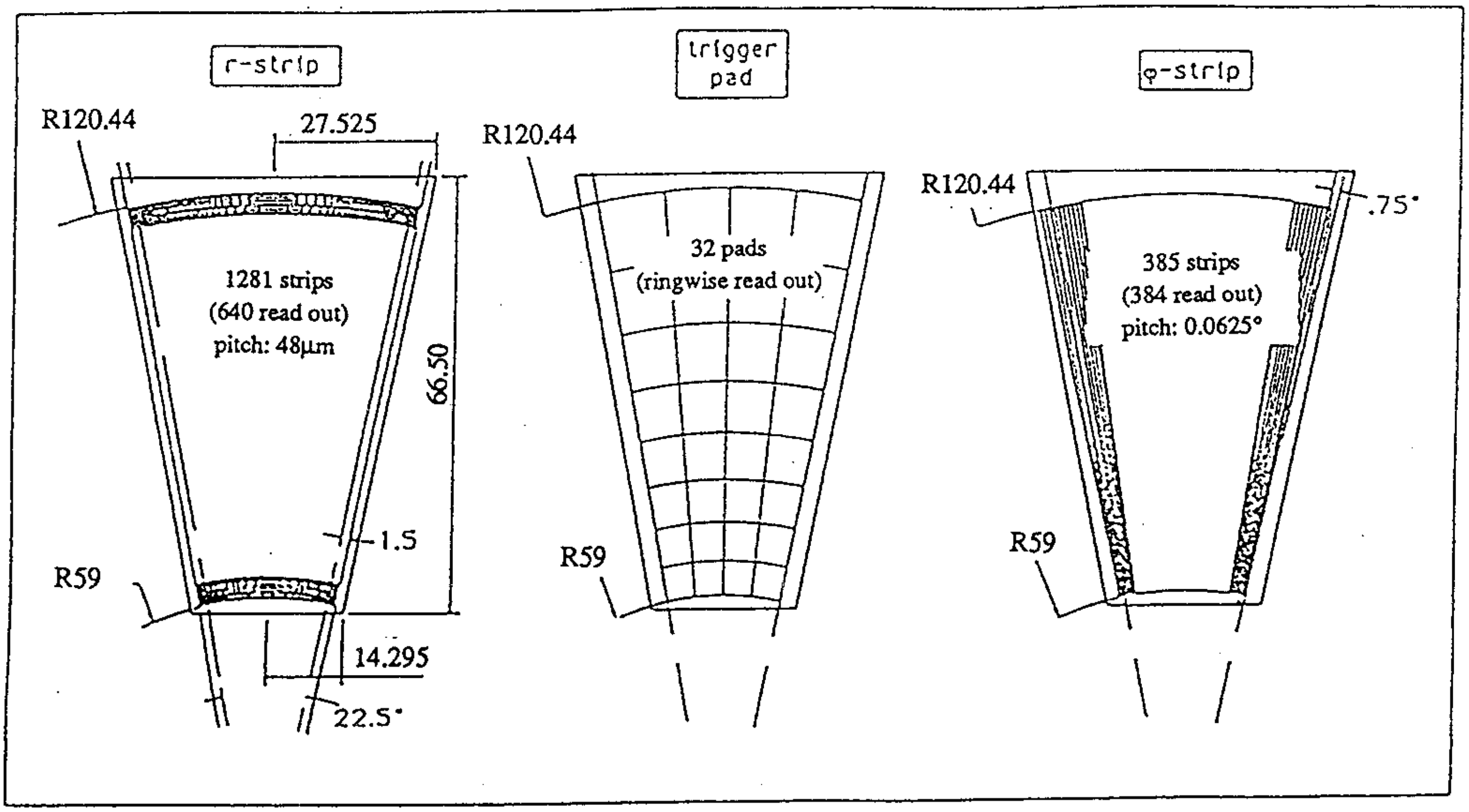

Figure 4: Three types of silicon sensors for BST - principle layout.

every possible position is filled with a detector plane. Optimization between maximum ϑ aperture and a wide plateau where a track crosses three or four planes leads to a 'best suiting' topology for BST(1) and (2), respectively, see fig. 6.

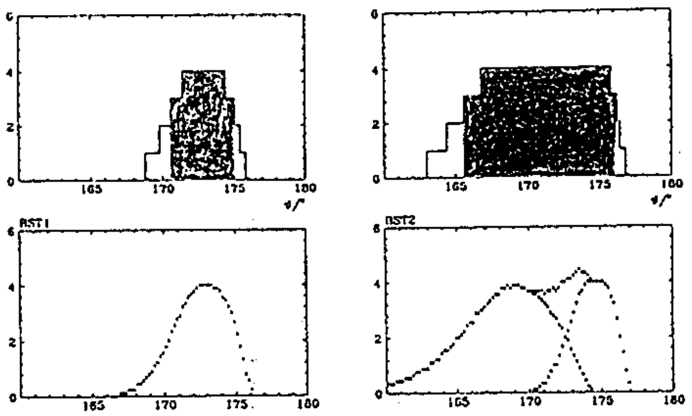

Figure 6: Polar angle acceptance for BST(1) (left) and BST(2) (right) with fix vertex (top) and with vertex smearing of ±100mm (bottom). The superimposition of the first and the second four planes of BST(2) is visualized. At least three hits are required for reconstruction of a track (darkened area).

The trigger principle is then to fit any event hit pattern to a set of predefined 'masks'. Nominally quite a little number of masks is enough to match straight tracks from a fixed vertex traversing through 3 or 4 planes. However, at HERA the vertex position varies over a few tens of cm due to the long proton bunches. A vertex position uncertainty of ± 1, 10 or $20cm$ increases the number of masks to 15, 48 or 57, resp. By simulation we found that genuine events produced more than 200 valid patterns, most of them occuring at a per mille rate however. It should therefore be possible to simplify the trigger logics without degrading the trigger performance noticeably.

We investigated four questions of major concern on the trigger logics complexity:

- *Which Granularity in ϕ is sufficient?*

The sensor shape imposes a 16fold azimuthal subdivision within a detector plane. In order to tag the scattered electron the trigger has to recognize an isolated charged track on its way through consecutive planes. We found that only 0.5% of the events in the energy range of interest have both the electron and a hadron track within the same $2\pi/16$ segment of the ϕ plane, thus preventing a successful tagging [3]. When we accept this trigger inefficiency we can handle each ring sector of the sensor as a single trigger channel.

- *How stiff are the tracks?*

The sensors of consecutive planes located at the same azimuthal position form a spatial sector. The question is: Will trigger information from within a given sector be sufficient for a stringent decision or are hits from adjacent sectors to be included in order not to place an arbitrary momentum cut? We did simulation on four subsequent planes (BST(1)) which show that down to a particle momentum of $2GeV$ there is no visible acceptance loss, if we require three passed planes only, i.e. if we allow the track to enter a given sector in the second plane or leave it after the third, see fig. 7. Apparently a BST(1) trigger may be built of 16 identical logic blocks, each one looking at the sensors of its own ϕ sector only (32 signals: 4 planes times 8 rings). For BST(2) it is foreseen so far to implement two individual 4-plane triggers and to link their track information together.

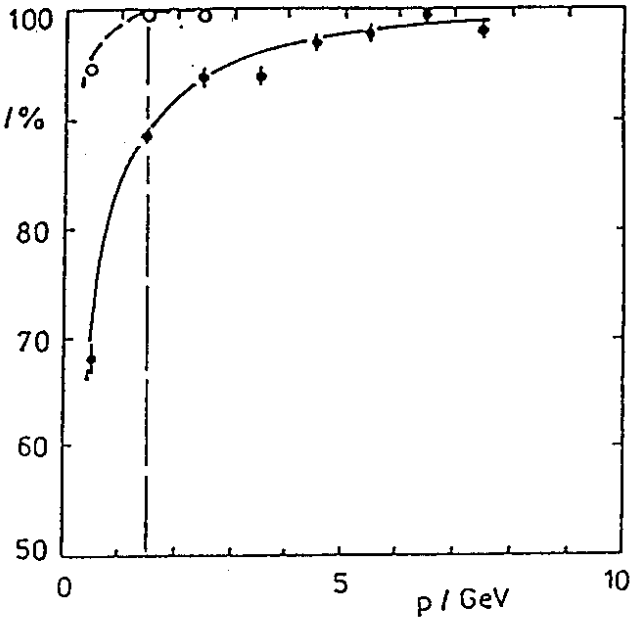

Figure 7: Fraction of charged tracks not leaving 1/16 of 2π while traversing through 4 and 3 consecutive BST planes (solid and dashed curve, resp.).

- *Which number of masks is reasonable?*

To implement a lot of rarely used patterns rises the acceptance rate but on the other hand it increases the probability to trigger on particle background or even on electronics noise. Our simulation showed that a reasonable trade-off between physics efficiency and background rejection rate can hardly be settled at once prior to knowing the performance conditions. Fig. 8 illustrates the decision latitute: For a vertex uncertainty of ± $20cm$ about 54 masks are necessary to reach 100% efficiency. At this level, however, a certain amount of background events, e.g. 6% of beam wall interactions and 2% of beam gas interactions, will pass the trigger already. Note, that the scale of the diagram is given by the frequency of occurrence of a specified pattern in a generated event sample. Most of those masks are rarely frequented.
The low number of masks and the independence of the 16 trigger blocks allows to implement the matching logics into a reconfigurable circuitry. Thus a suitable number of masks together with possible arbitrary patterns to cope with sensor faults or degradations due to radiation exposure can be generated and loaded for each and every performance condition.

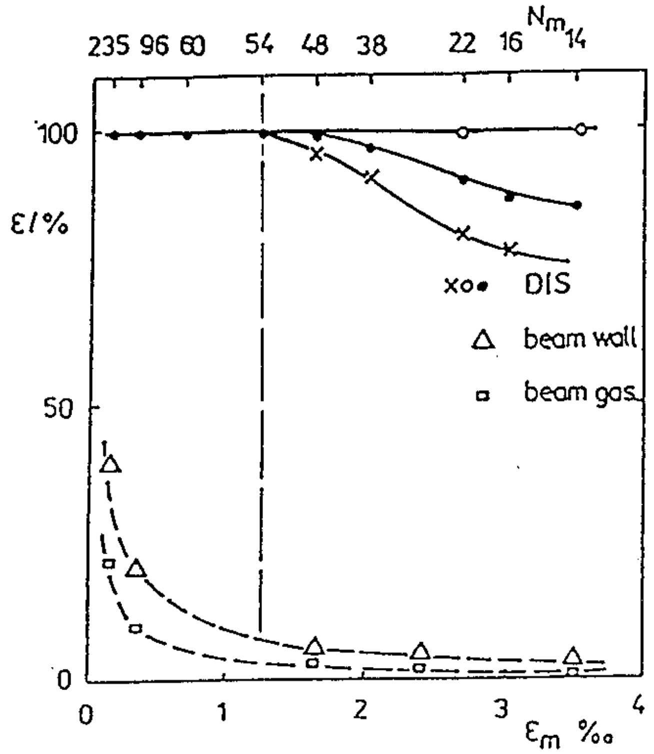

Figure 8: Trigger efficiency as a function of the number of allowed hit patterns ('masks'), being met with a frequency of less than ε_m per mille (abscissa). With vertex smearing the number of required patterns increases (circles: ±0, dots: ±10cm, crosses: ±20cm), however also a considerably greater fraction of background events meets the trigger condition.

- *What about rates?*

When we consider realistic rates it turns out that background rejection power is rather vital for the trigger concept at all. While the deep inelastic event rate is expected at about *1Hz* background events will have matching tracks at a two orders of magnitude higher rate. Though the trigger will thus have to be combined with Time-of-Flight Veto and with the backward calorimeter it is highly desirable to apply an additional, background specific cut to the mask matching process. This may easily be a hit multiplicity check: While both physics and background events peak at about 5 hits in the BST(1) only the beam wall and the beam gas interactions result in multiplicities above 20 (12% and 17% resp.). The implementation of an additional cut on the number of hits reduces faked triggers by a factor of 2 (beam wall) and 3 (beam gas), see fig. 9.

3.2 Sensor Design & Prototyping

3.2.1 Strip Detectors

The principal layout of the different detectors is shown in fig. 4. The strip detectors will be read out by an on purpose developed preamplifier/pipeline integrated circuit [4]. This preamplifier requires AC coupled detectors with integrated biasing. The bonding area is to be located at the outermost edge of the pie; so the ϑ detectors must have a double metallization layer which connects the circular strips to the row of bonding pads, see fig. 10. The strip pitch is $48\mu m$ in radius (every second one read out) and 1/16 degree in ϕ, respectively, and the total number of channels per sensor amounts to 640 and 384. Recently ϑ detectors have been prototyped which are now under investigation.

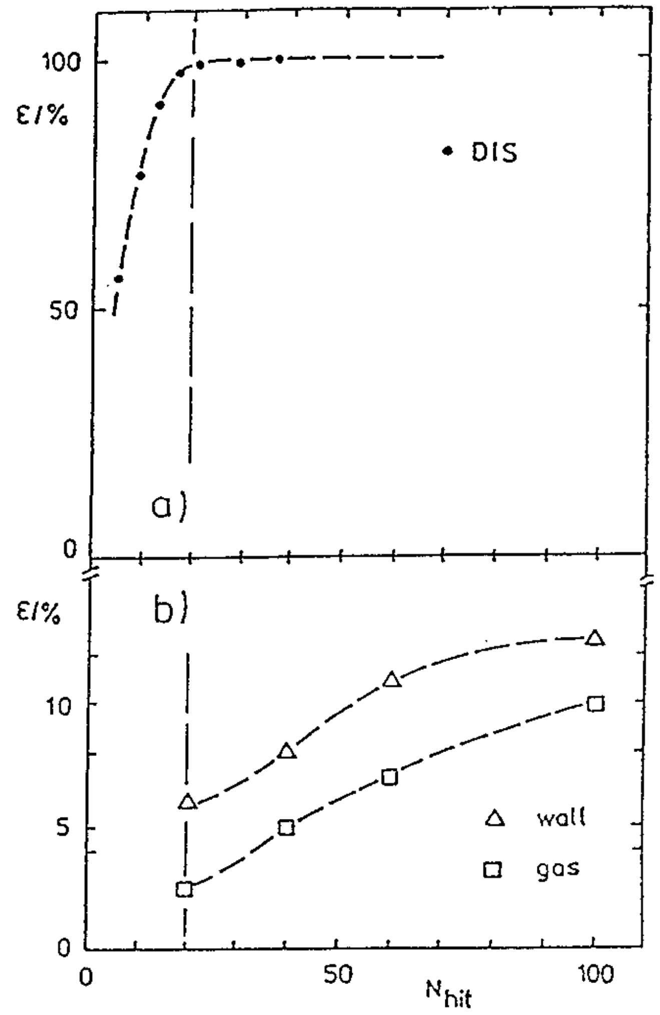

Figure 9: Trigger efficiency as a function of the total hit multiplicity in the BST (4 planes). A cut at $N_{hit} = 20$ only marginally affects the trigger performance.

3.2.2 Trigger Detectors

The trigger sensors show a pattern of diodes shaped to ring segments (so called 'pads'), fig. 11. Every one of the 'logical' 8 rings is subdivided into 4 individual pads in order to reduce its overall capacitance. The pad size varies by about an order of magnitude (1:12), the capacitance between $7pF$ and about $50pF$ (measured on prototypes). The diodes will be biased through the preamplifier input stage. Due to the large size of the structure elements every local process fault would affect a noticeable percentage of the signal channels. So we chose a rather simple design with DC coupled diodes which are connected to the bonding pads by tracks in a single metallization layer. The detector prototypes show a good yield: Only 3.5% of totally 256 tested pads had some kind of malfunction.

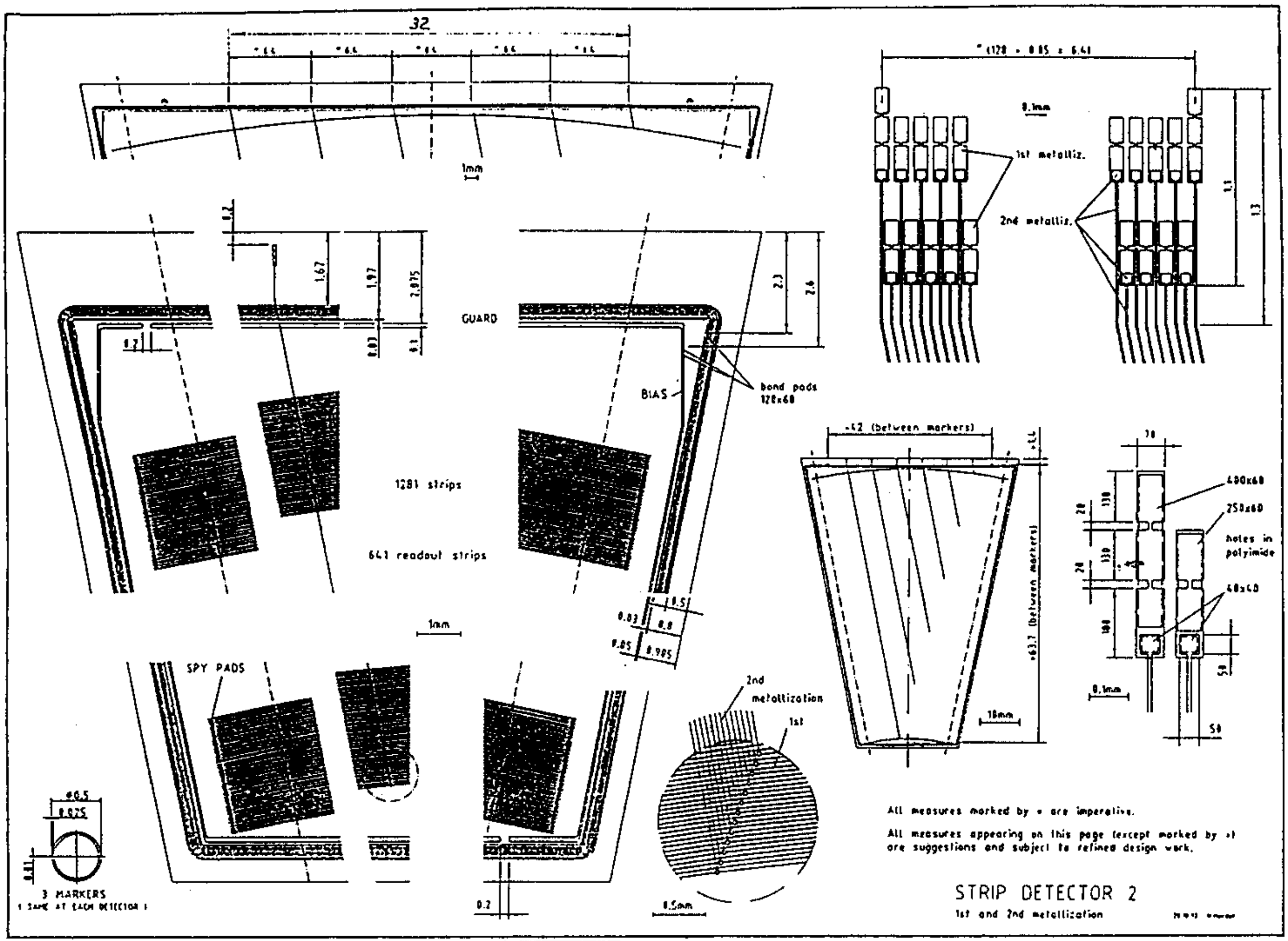

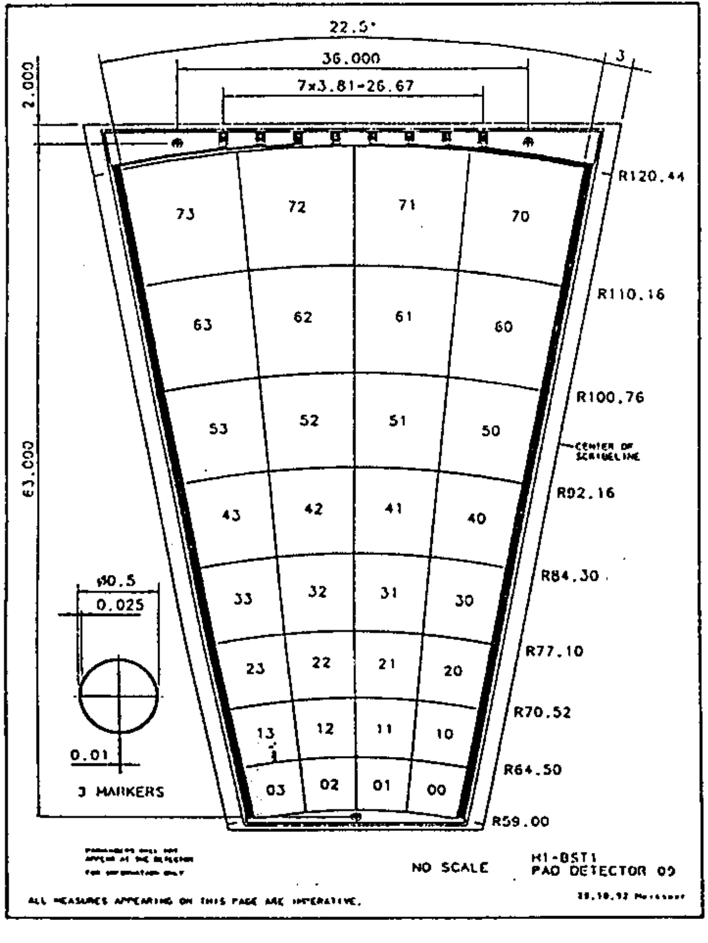

Figure 10 (top): Layout of the ϑ strip detector. The circular inset shows how the diode strips are connected to the readout tracks (second metallization). The sketch top right details the bonding pad array.

Figure 11 (left): Layout of the pad detector. The wide black surrounding of the 32 diode pads is an area of tracks connecting each diode to a bonding pad in the row of 8 arrays near the top edge.

4. ELECTRONICS

4.1 Trackers

The BST tracker readout and data aquisition are essentially the same as of the likewise proposed Central Silicon Tracker being described elsewhere [1,5]. Here we only mention that every ϑ sensor will be equipped with 5 preamplifier/multiplexer chips, every ϕ sensor with 3 of them. The total number of signal channels is $4 \cdot 10^4$ for BST(1) and $13 \cdot 10^4$ for BST(2).

4.2 Trigger

The trigger sensors provide 32 diode signals each, which are amplified and discriminated by an integrated 4 channel chip currently being developed. Main emphasize will be payed to

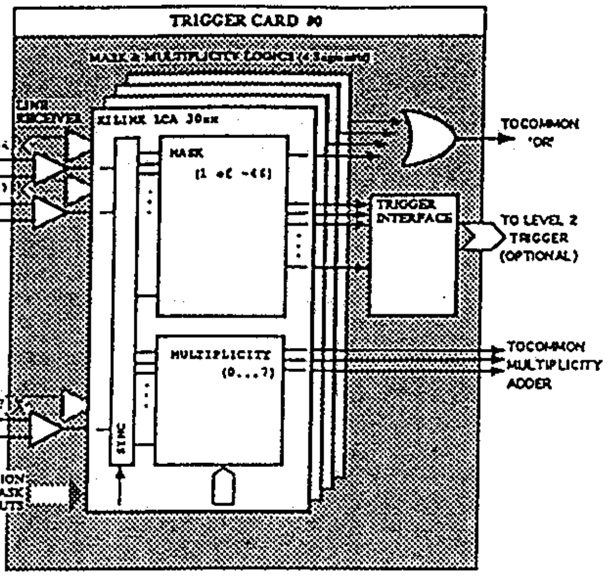

Figure 12: The Trigger Card, principle design. It implements synchronisation, masking and multiplicity cut on 4 ϕ segments of the BST (4 planes).

a short (45*ns*) peaking time despite a high capacitive input load [6]. The digital outputs of the four pads of every ring will be ORed together and transmitted in parallel to the trigger frontend logics, amounting to 512 channels in total for BST(1) and to 1024 for BST(2). Field programmable logic will synchronize the trigger signals to the common HERA machine clock and then check the hit patterns against a set of up to about 60 predefined masks. Additionally an adjustable multiplicity cut can be invoked. Simulation showed that for just 4 consecutive planes those three tasks easily fit into a single XILINX LCA series 3000 chip per ϕ sector. It is foreseen to add an extension input to every mask which will allow to link valid tracks of the first four planes to those of the second four in the fully equipped BST(2). Independent trigger decisions of any sectors are then ORed to a common level 1 trigger output, and as an option every sector may store its hit pattern in a pipeline for use by the central trigger logics at level 2, see fig. 12. Due to its fully parallel design this trigger is deadtime free and leaves plenty of time for combination with other triggers in the H1 central trigger circuitry.

Obviously a sensor bias supply and test pulse circuitry will be incorporated.

5. MECHANICS

The BST will be set up on a carbon fibre framework, consisting of spoke wheels and plinths, see fig. 13. The wheels have precision machined surfaces to which the sensors are mounted by support of small multilayer hybrids. Microscope survey and adjustment ensure exact centricity of the wedges within every wheel. Since the whole BST will be enclosed by Faraday shields a water cooling system removes about 40*W* of dissipated energy. The detector is detachable into two independent halves which slide over the beam pipe thus avoiding the need for a vacuum break upon assembly.

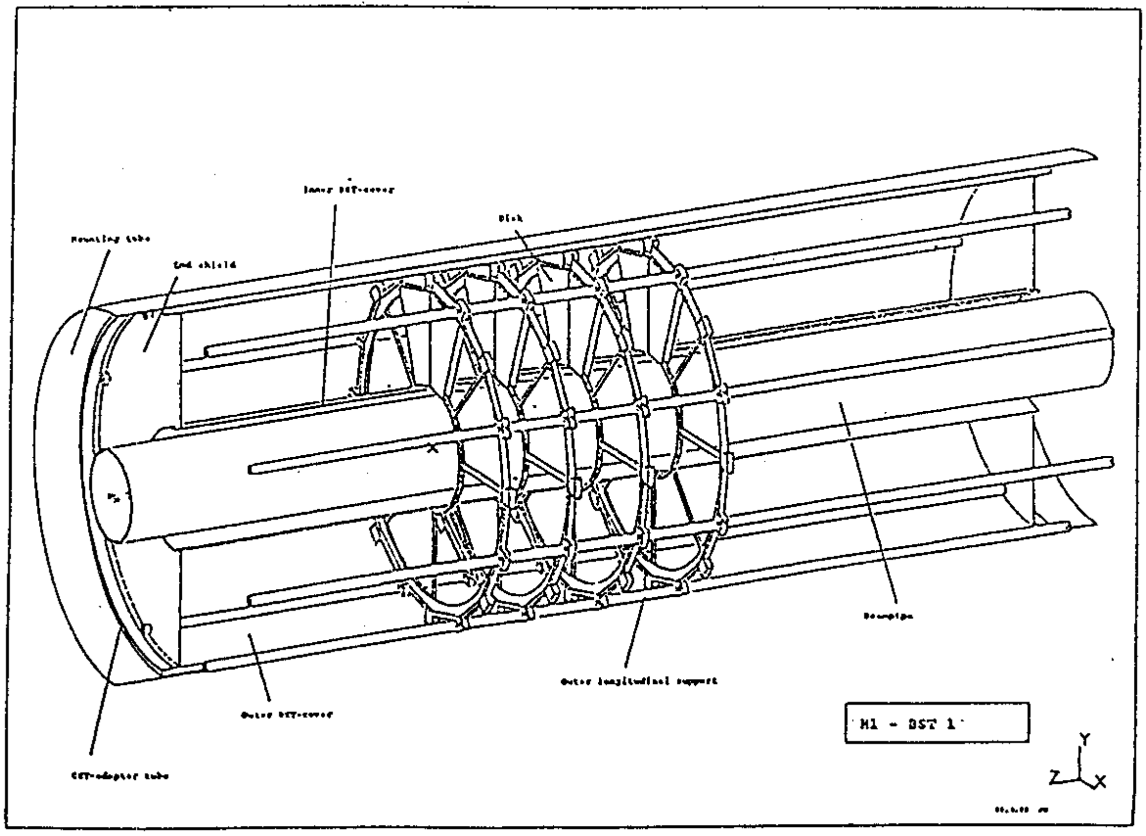

Figure 13: BST(1) perspective view with beam pipe, spoke wheels and shieldings. On top of the beam pipe two adjacent sensor pies in two layers are visible.

6. SUMMARY

The Backward Silicon Tracking detector (BST) for the HERA experiment H1 will consist of 8 planes (stage 1, 1994: 4 planes) perpendicular to the beam in distances from the vertex between 300*mm* and 1046*mm* and covering the radial clearance between the beam pipe and the innermost existing tracking detector ($r = 59\ldots120.4mm$). The planes will be equipped with three types of silicon sensors, two for track measurements (ϑ and ϕ to 1*mrad* each) and one for triggering on charged particles. Detector prototypes are under test. The BST will finally comprise about 10^5 analog readout channels and 1024 parallel trigger channels. A monolithic amplifier/discriminator for high-capacitive diode readout is being developed. The incorporated pointing track trigger will in conjunction with improved backward calorimetry allow to tag deep inelastic events and to reduce beam background trigger rates.

7. ACKNOWLEDGEMENTS

We wish to express our gratitude to R. Horisberger, E. Nygård, D. Pitzl, P. Weilhammer and W. Zimmermann for valuable discussions and suggestions and to B. Avset at SI Oslo for intense collaboration on the prototype design.

8. REFERENCES

[1] H1 Collaboration: "Technical Proposal to build Silicon Tracking Detectors for H1." DESY Internal Notes PRC 92/01 & H1 06/92-226, July 1992.

[2] H1 Collaboration: "Expression of Interest to upgrade the Backward Electromagnetic Calorimeter." DESY Internal Notes PRC 92/03 & H1 09/92-243, September 1992.

[3] H.Henschel et al. "A Silicon Pad Detector L1 Trigger for Deep Inelastic Scattering at Low x and Q^2." DESY Internal Note H1 04/92 - 221, April 1992.

[4] R. Horisberger, D. Pitzl: "A New Amplifier and Pipeline Chip for Silicon Strip Detector Readout." Talk presented at the Nuclear Science Symposium, Orlando, Florida, October 1992.

[5] K. Gabathuler et al. "A Silicon Vertex Detector for H1 at HERA." Talk presented at the Nuclear Science Symposium, Orlando, Florida, October 1992.

[6] Design basing on preamplifiers of E.Nygård et al., "CMOS low noise monolithic frontends for Si strip detector readout.", Contribution to the Milano Conference on semiconductor detectors, Milano, 1992.